

Siloxane-terminated phenylpyrimidine liquid crystal hosts†

Li Li,^a Christopher D. Jones,^b Jakob Magolan^a and Robert P. Lemieux^{*a}

Received 22nd January 2007, Accepted 5th March 2007

First published as an Advance Article on the web 21st March 2007

DOI: 10.1039/b700972k

We report the synthesis and characterization of trisiloxane-terminated liquid crystals with 2-phenylpyrimidine cores that form partially bilayered SmA and SmC phases. Variable temperature measurements of smectic layer spacings by powder X-ray diffraction combined with measurements of optical tilt angles and observations of birefringence changes by polarized optical microscopy reveal that the trisiloxane end-group causes the SmA–SmC transition of these compounds to be more ‘de Vries-like’ when compared to a non-siloxane analogue. One such compound, 2-(4-(11-(1,1,1,3,3,5,5-heptamethyltrisiloxanyl)undecyloxy)phenyl)-5-(1-chlorooctyloxy)pyrimidine (**3**), is characterized by a maximum layer shrinkage of only 1.6% and may be considered a *bona fide* de Vries material.

Introduction

Nanosegregation plays a key role in the self-organization of liquid crystal phases. In the condensed phase, amphiphilic molecules containing two or more incompatible segments self-organize due to the segregation of these segments into distinct domains on the nanometer scale with topographies dictated by the molecular shape and the amphiphilic interface curvature.¹ Conventional calamitic (rod-shaped) molecules consisting of a rigid aromatic core and two paraffinic side-chains form lamellar smectic phases due, in part, to the difference in conformational rigidity between aromatic and paraffinic segments. Whereas the amphiphilicity of conventional calamitic mesogens is rather subtle, the formation of lamellar mesophases can be strongly promoted by the design of calamitic mesogens with more pronounced amphiphilicity combining, for example, hydrophilic and lipophilic segments, fluorocarbon and hydrocarbon segments, or siloxane and hydrocarbon segments. Amphiphilicity and nanosegregation can also be used to compatibilize non-mesogenic dopants with liquid crystal hosts. Coles and co-workers demonstrated this concept with a combination of non-mesogenic dichroic dye and smectic liquid crystal host molecules, both terminated with short siloxane oligomers.^{2–4} The addition of a siloxane end-group to a calamitic mesogen has been shown to promote lamellar organization and the formation of smectic phases due to the tendency of siloxane and paraffinic groups to nanosegregate into distinct sublayers,^{5–14} forming a so-called ‘virtual siloxane backbone’ that enables dopant compatibilization in a way similar to what is achieved with side-chain liquid crystalline copolymers.¹⁵

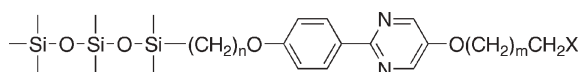
An interesting aspect of amphiphilic molecules such as siloxane-terminated smectogens is the reduced degree of out-of-layer fluctuations, and the added control of core–core correlation in the smectic layer that is afforded by siloxane nanosegregation. Such control is particularly relevant to our ongoing studies of chirality transfer *via* core–core interactions in ferroelectric SmC* liquid crystals induced by chiral dopants with atropisomeric biphenyl cores.^{16,17} We have shown that the chiral perturbations exerted by these atropisomeric dopants are propagated most effectively in an achiral liquid crystal host with a complementary 2-phenylpyrimidine core structure, leading to enhanced ferroelectric polarizations in the chiral SmC* phase. Hence, the ability to tune core–core interactions by varying the length of the side-chain linking siloxane end-groups to the cores of both dopant and phenylpyrimidine host would enable one to probe the effect of chirality transfer *via* core–core interactions more systematically. More recently, we have shown that one particular atropisomeric dopant induces a remarkably high electroclinic effect in the chiral SmA* phase using the same phenylpyrimidine liquid crystal host.¹⁸

Yet another interesting aspect of some amphiphilic compounds, including both siloxane-terminated mesogens and mesogens with perfluorinated side-chains, is the formation of ‘de Vries’ SmA* phases, which are characterized by a tilted molecular orientation with random azimuthal distribution.^{19–25} These materials experience minimal layer shrinkage upon transition to the ferroelectric SmC* phase, which minimizes the formation of chevrons and zigzag defects that severely degrade the quality of electro-optic devices based on ferroelectric liquid crystal materials.²⁶ Surprisingly, despite the ubiquitous nature of phenylpyrimidine liquid crystals in ferroelectric liquid crystal (FLC) mixture formulations, examples of siloxane-terminated phenylpyrimidine mesogens have yet to be reported. In this paper, we report the synthesis and characterization of trisiloxane-terminated liquid crystals with 2-phenylpyrimidine cores that form partially bilayered SmA and SmC phases (**1–8**), and present evidence suggesting that the SmA phase formed by some of these compounds has de Vries character.

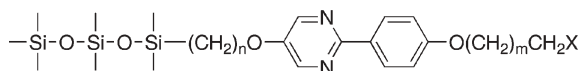
^aChemistry Department, Queen's University, Kingston, Ontario, K7L 3N6, Canada

^bDepartment of Physics, University of Colorado at Boulder, Boulder, CO, 80309, USA

† Electronic supplementary information (ESI) available: synthetic procedures and spectral characterization data (¹H and ¹³C NMR, low- and high-resolution MS) for all new compounds, thermal analysis data and optical tilt angle plots. See DOI: 10.1039/b700972k



- 1, X=H, n=11; **a**, m=6; **b**, m=7; **c**, m=8; **d**, m=9; **e**, m=11
 2, X=H, n=6; **a**, m=6; **b**, m=7; **c**, m=8; **d**, m=9; **e**, m=11
 3, X=Cl, n=11, m=7
 4, X=Cl, n=6, m=7



- 5, X=H, n=11, m=7
 6, X=H, n=6, m=7
 7, X=Cl, n=11, m=7
 8, X=Cl, n=6, m=7

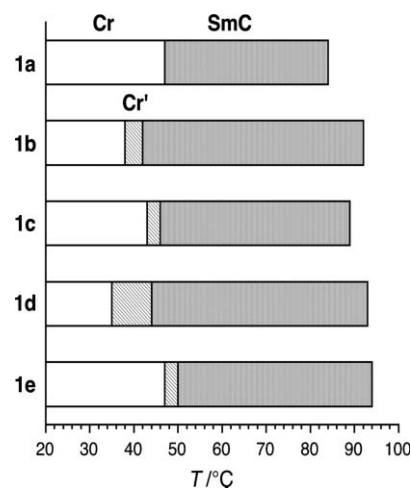


Fig. 1 Phase transition temperatures for compounds **1a–e** measured by DSC on heating.

Results and discussion

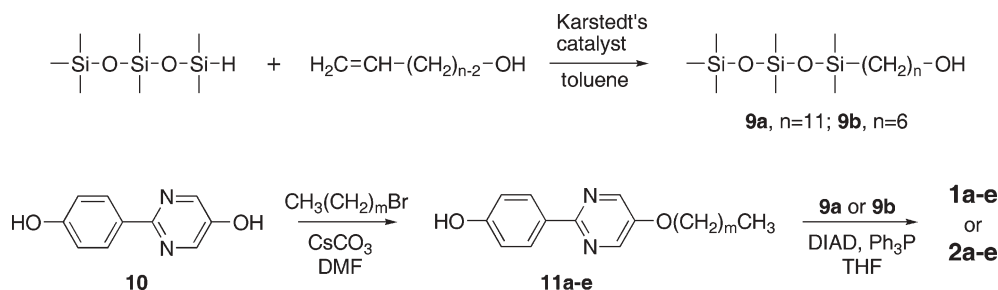
Synthesis

All siloxane-terminated phenylpyrimidine liquid crystals reported herein were prepared by sequential alkylations of 2-(4-hydroxyphenyl)-5-pyrimidinol (**10**). As shown in Scheme 1, the synthesis of compounds **1** and **2** began with the selective alkylation of **10** under basic conditions to give the 2-(4-hydroxyphenyl)-5-alkoxy-pyrimidine precursors **11a–e** in 61–65% yield. The siloxane-terminated alcohols **9a** and **b** were prepared from 10-undecen-1-ol and 5-hexen-1-ol, respectively, *via* a platinum-catalyzed hydrosilylation reaction using 1,1,1,3,3,3,5,5-heptamethyltrisiloxane and either dicyclopentadienylplatinum(II) chloride or Karstedt's catalyst in 80–95% yield, and then combined with **11a–e** *via* a Mitsunobu reaction to give **1a–e** and **2a–e** in yields ranging from 46 to 52%. The 'inverted' phenylpyrimidine liquid crystals **5** and **6** were prepared by simply reversing the alkylation sequence shown in Scheme 1. The terminal chlorooctyloxy analogues **3** and **4** were prepared by alkylation of **10** *via* a Mitsunobu reaction with 8-chloro-1-octanol in 52% yield, followed by alkylation with **9a** and **9b**, respectively. The inverted analogues **7** and **8** were prepared by reversing the alkylation sequence.

Mesophase characterization

The mesophases formed by compounds **1–8** were characterized by polarized optical microscopy (POM), differential scanning calorimetry (DSC) and powder X-ray diffraction (XRD). Compounds **1a–e** form a single mesophase showing both

broken fan and Schlieren textures by POM, which are characteristic of a tilted SmC phase (Fig. 1, and Table S1 in ESI†). DSC analysis revealed, in some cases, a second melting transition (Cr–Cr') on heating, which has been attributed previously to the melting of siloxane domains separate from that of paraffinic domains.^{7,10} The phase transition temperatures in series **1a–e** show a relatively subtle odd–even effect with respect to the alkoxy chain length. The powder XRD profiles of these compounds are consistent with a disordered smectic phase; they show first and second-order Bragg diffraction peaks in the small-angle region corresponding to the smectic layer structure, together with a pair of diffuse bands in the wide-angle region corresponding to the disordered lateral arrangement of paraffinic chains (4.5 Å) and siloxane groups (6.9 Å) within each layer (for a representative example, see Fig. 2).^{4,9,10} In the case of compound **1b**, the Bragg angle 2θ in the small-angle region corresponds to a layer spacing d of 43.5 Å, which is slightly longer than the molecular length of **1b** (see Table 1) and therefore inconsistent with a tilted lamellar structure. Such a discrepancy between the X-ray data and POM observations has been previously reported for other siloxane-terminated liquid crystals, and rationalized by the formation of a partially bilayered SmC structure.^{9,10} We attempted to measure the optical tilt angle of the SmC phase by POM using a sample of **1b** doped with the chiral siloxane **Br11-Si₃** (1 mol%),¹⁰ but were unable to achieve a uniform alignment of the SmC* mixture in ITO cells (*ca.* 1 μm spacing) with either rubbed polyimide or rubbed Elvamide[®] alignment layers.



Scheme 1



Shortening the alkyl spacer linking the siloxane end-group to the phenylpyrimidine core (series **2a–e**) resulted in the formation of a very narrow SmA phase along with the broader SmC phase (Fig. 3). These results are consistent with normally observed trends showing a stabilization of the SmC phase at the expense of the SmA phase with increasing chain length. The SmA phase was distinguished from the SmC phase by POM observations of coexisting domains with fan and homeotropic textures (SmA) which turned into broken fan and Schlieren textures upon transition to the SmC phase. Accurate measurements of smectic layer spacings as a function of temperature by powder XRD were carried out for compound **2b**. As shown in Fig. 4, the SmA–SmC phase transition results in a maximum layer shrinkage of 7.6%, which is within the range of conventional materials with this phase sequence.²⁶ The d spacing in the SmA phase of compound **2b** is longer than the calculated molecular length by 3.9 Å (see Table 1), which is consistent with the assignment of a partially bilayered structure. Unlike the previous case, we were able to achieve a uniform alignment of a 1 mol% mixture of **Br11-Si₃**

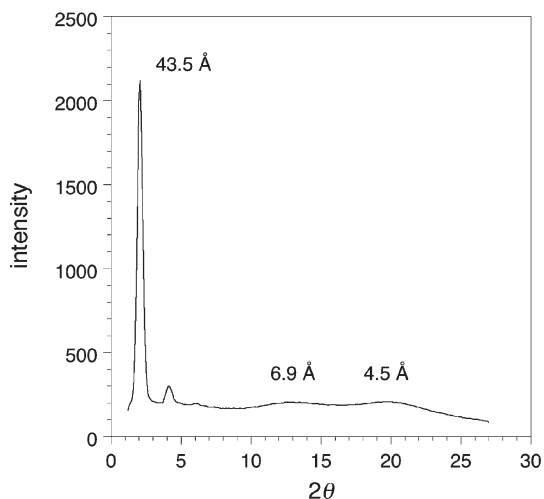


Fig. 2 Powder X-ray diffraction profile for compound **1b** in the SmC phase.

Table 1 Smectic layer spacings in the SmA phase (d_A) and SmC phase (d_C) at $T - T_C = -10$ K, molecular lengths derived from AM1 molecular modeling (L), optical tilt angles (θ_{opt}) measured by POM, and de Vries coefficients (C_{dV}) at $T - T_C = -10$ K

| Cpd | $d_A/\text{Å}$ | $d_C/\text{Å}$ | $L/\text{Å}$ | $\theta_{\text{opt}}/\text{deg}^a$ | C_{dV}^b |
|-----------|----------------|----------------|--------------|------------------------------------|------------|
| 1b | — | 43.5 | 42.3 | — | — |
| 2b | 39.6 | 36.9 | 35.7 | 36 | 0.64 |
| 3 | 48.4 | 47.7 | 42.8 | 24 | 0.83 |
| 4 | 40.4 | 38.9 | 36.2 | 26 | 0.63 |
| 5 | — | 35.8 | 42.3 | — | — |
| 6 | — | 28.3 | 35.7 | — | — |

^a Measured with samples containing 1 mol% of **Br11-Si₃**.

^b Calculated using eqn (3) and maximum d_A value at T_C .

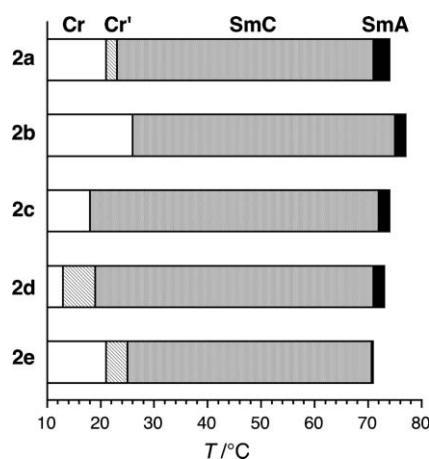


Fig. 3 Phase transition temperatures for compounds **2a–e** measured by DSC on heating.

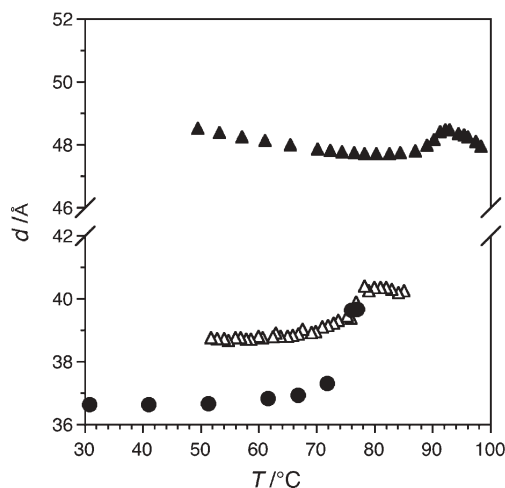


Fig. 4 Smectic layer spacing d vs. temperature T for compounds **2b** (circles), **3** (filled triangles) and **4** (open triangles).

in **2b** in an ITO cell with rubbed Elvamide[®] alignment layers, which enabled the measurement by POM of an optical tilt angle of 36° at $T - T_C = -10$ K.

We sought to modify the molecular structure of these compounds to broaden the range of the SmA phase because of the proven potential of siloxane-terminated mesogens to form de Vries SmA phases.^{19–23} Based on a recent report by Cowlings *et al.* that the inclusion of a terminal halogen atom in the side-chain of a calamitic mesogen promotes the formation of a SmA phase,²⁷ we modified the side-chains of both **1b** and **2b** to give the chloro-terminated mesogens **3** and **4**. As shown in Fig. 5, the inclusion of a terminal chloro substituent resulted in narrower SmC temperature ranges, and broader SmA temperature ranges of 9 K in both cases. As observed with series **1** and **2**, layer spacings in the orthogonal and tilted smectic phases are longer than the corresponding molecular lengths (Table 1), which is consistent with the assignment of partially intercalated bilayer structures. The SmA–SmC phase transition results in a maximum layer shrinkage of 4.2% for compound **4** and only 1.6% for compound **3**, although the d_C spacing of **3** increases with decreasing temperature to such an

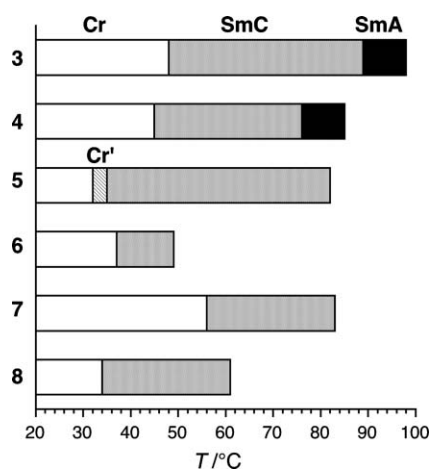


Fig. 5 Phase transition temperatures for compounds **3–8** measured by DSC on heating.

extent that $d_C = d_A$ near the SmC–Cr transition (Fig. 4). The $d(T)$ profile for compound **3** is very similar to that reported for one of the perfluorinated 3M materials with a ‘de Vries’ SmA*–SmC* transition that results in a maximum layer shrinkage of 0.8%.²⁴ The effect of the terminal chloro substituents in promoting orthogonal layer structures is reflected in smaller optical tilt angles of 24 and 26° at $T - T_C = -10$ K in the SmC phases of **3** and **4**, respectively. We also observed significant changes in interference colors in the fan/broken fan textures of both **3** and **4** upon cooling from the SmA to the SmC phase (Fig. 6 and 7). These color changes indicate an increase in birefringence that is expected

in a ‘de Vries’ phase transition from random to ordered molecular tilt (*vide infra*).²⁶

To assess whether the decrease in layer shrinkage achieved by introducing a terminal chloro substituent in the side-chain of **2b** is due to an increase in ‘de Vries’ character, one must consider the difference in tilt angle in the SmC phases formed by these materials. The description of any SmA–SmC phase transition may be found somewhere along a continuum between two limiting cases, the classic rigid rod model (Fig. 8a) and the diffuse cone model proposed by de Vries (Fig. 8b).^{26,28} According to the first model, in which rigid rod molecules are uniformly oriented along a director \mathbf{n} and tilted at an angle θ with respect to the layer normal \mathbf{z} , the relationship between d_C and d_A is expressed by eqn (1), and the layer shrinkage $(d_A - d_C)/d_A$ is a function of the tilt angle θ according to eqn (2). In order to attribute any decrease in layer shrinkage to an increase in ‘de Vries’ character based on the diffuse cone model, we normalize the layer shrinkage with respect to θ by dividing the observed $(d_A - d_C)/d_A$ by $1 - \cos\theta$, where θ is approximated as the optical tilt angle θ_{opt} measured by POM (eqn (3)). Using this expression, the ‘de Vries’ coefficient C_{dV} of any given material can range from 0 (classic rigid rod model with maximum layer shrinkage) to 1 (pure ‘de Vries’ SmA–SmC transition with no layer shrinkage).

$$d_C = d_A \cos\theta \quad (1)$$

$$(d_A - d_C)/d_A = 1 - \cos\theta \quad (2)$$

$$C_{\text{dV}} = 1 - [(d_A - d_C)/(d_A(1 - \cos\theta))] \quad (3)$$

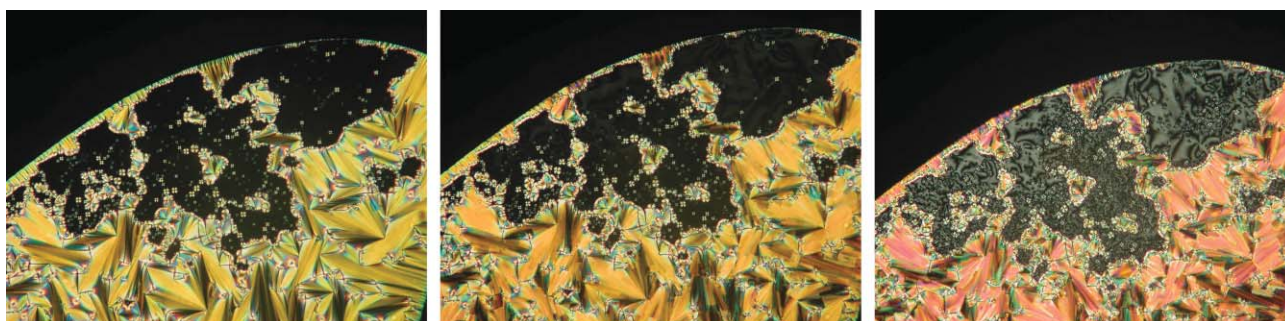


Fig. 6 Polarized photomicrographs of compound **3** on cooling: in the SmA phase at 91 °C (left), just below the SmA–SmC phase transition at 86 °C (middle), and in the SmC phase at 82 °C (right).

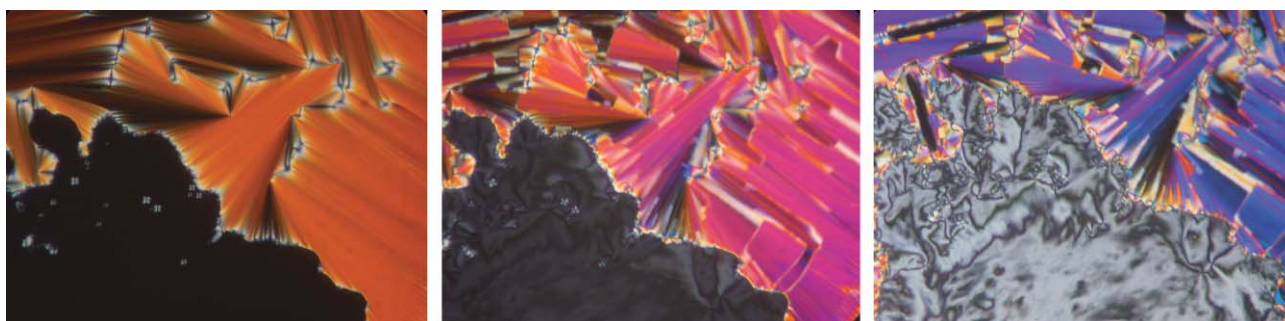


Fig. 7 Polarized photomicrographs of compound **4** taken on cooling: in the SmA phase at 82 °C (left), just below the SmA–SmC phase transition at 73 °C (middle), and in the SmC phase at 62 °C (right).

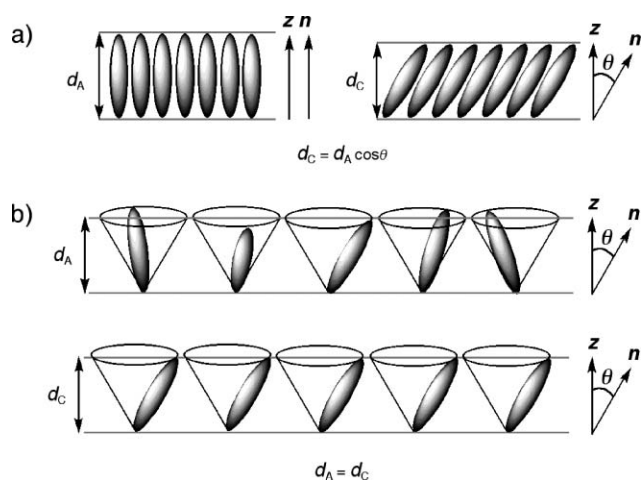


Fig. 8 Schematic representations of the SmA–SmC phase transition according to (a) a classic rigid-rod model and (b) a ‘de Vries’ diffuse cone model.²⁸

Optical tilt angles θ_{opt} were measured as a function of temperature by POM using 1 mol% mixtures of **Br11-Si₃** in **2b**, **3** and **4**, and used to calculate C_{dV} values over the SmC temperature range of each mesogen.²⁹ As shown in Fig. 9, the C_{dV} of compound **2b** shows little variance with temperature, with values ranging from 0.63 to 0.67. By comparison, the non-siloxane analogue **PhP1** has a C_{dV} value of 0.40 at $T - T_{\text{C}} = -10$ K,¹⁸ which suggests that the trisiloxane end-group does impart some ‘de Vries’ character to the SmA–SmC transition of compounds in series **2**. The $C_{\text{dV}}(T - T_{\text{C}})$ profile of compound **4** is steeper than that of **2b**, although C_{dV} values are fairly similar in the $T - T_{\text{C}}$ range of -5 to -15 K. At $T - T_{\text{C}} = -10$ K, the two compounds have nearly the same C_{dV} value despite the large difference in layer shrinkage (6.8% vs. 3.7%, respectively) because of the difference in tilt angle. The $C_{\text{dV}}(T - T_{\text{C}})$ profile of compound **3** is similar to that of **4**, but features significantly higher C_{dV} values. With a maximum layer shrinkage of 1.6% and a C_{dV} of 0.89 at $T - T_{\text{C}} = -10$ K,

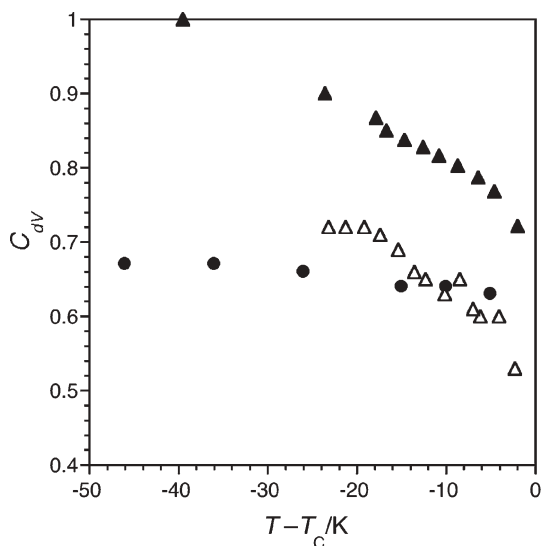
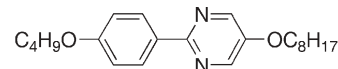


Fig. 9 De Vries coefficient C_{dV} vs. reduced temperature $T - T_{\text{C}}$ for compounds **2b** (filled circles), **3** (filled triangles) and **4** (open triangles).

compound **3** may be considered a *bona fide* ‘de Vries’ material with a SmA–SmC transition approaching that described by the diffuse cone model.^{19–25} However, given the partially bilayered structure of the smectic phases formed by these compounds, one cannot rule out a variation in the degree of bilayer intercalation as a contributor to the observed reductions in layer shrinkage.



PhP1: Cr 58 SmC 85 SmA 95 N 98 I

As shown in Fig. 5, inverting the orientation of the phenylpyrimidine core in compounds **5–8** resulted in a complete suppression of the SmA phase and a reduction in layer spacing d_{C} (Table 1), which is remarkable considering the fact that both side-chains are linked to the core *via* alkoxy groups, and that their conformational hypersurfaces should therefore remain unaffected by the inversion. The reduced layer spacing may reflect an increase in tilt angle, although we were unable to measure θ_{opt} with samples doped with **Br11-Si₃** due to extremely poor alignment of the SmC* phases in ITO cells with either rubbed polyimide or rubbed Elvamide[®] alignment layers. It may also reflect specific core–core interactions in the intercalated bilayer structure that are controlled primarily by π -stacking of the electron-poor pyrimidine rings, thus causing a shift in offset upon inverting the orientation of the cores.

Summary

The addition of a trisiloxane end-group on one side-chain of a dialkoxyphenylpyrimidine mesogen results in the formation of a broad SmC phase and, in some cases, a narrower SmA phase. The temperature range of the SmA phase may be broadened by the addition of a terminal chloro substituent on the other alkoxy side-chain. Measurements of d spacings and optical tilt angles as a function of temperature, combined with observations of changes in birefringence by polarized optical microscopy, revealed that the trisiloxane end-groups cause the SmA–SmC transitions of these compounds to be more ‘de Vries-like’. This is consistent with the notion that nanophase segregation plays a significant role in the manifestation of ‘de Vries’ behavior, whether it is achieved with amphiphilic mesogens,^{19–25} or with side-chain siloxane copolymers.³⁰ One compound, 2-(4-(11-(1,1,1,3,3,5,5-heptamethyltrisiloxanyl)undecyloxy)phenyl)-5-(1-chlorooctyloxy)pyrimidine (**3**), is characterized by a maximum layer shrinkage of only 1.6% and may be considered a *bona fide* de Vries material with the potential of exhibiting interesting ferroelectric and electroclinic properties upon doping with chiral materials. The use of this compound as liquid crystal host in the induction of ferroelectric and electroclinic properties is currently under investigation.

Acknowledgements

We are grateful to the Natural Sciences and Engineering Research Council of Canada, the Canada Foundation for

Innovation and the National Science Foundation (MRSEC grant DMR-0213918) for support of this work.

References

- C. Tschierske, *J. Mater. Chem.*, 1998, **8**, 1485; J. W. Goodby, G. H. Mehl, I. M. Saez, R. P. Tuffin, G. Mackenzie, R. Auzély-Velty, T. Benvegnu and D. Plusquellec, *Chem. Commun.*, 1998, 2057; C. Tschierske, *J. Mater. Chem.*, 2001, **11**, 2647; C. Tschierske, *Annu. Rep. Prog. Chem., Sect. C: Phys. Chem.*, 2001, **97**, 191.
- D. Shoosmith, C. Carboni, S. Perkins, S. Meyer and H. J. Coles, *Mol. Cryst. Liq. Cryst.*, 1999, **331**, 181.
- D. E. Shoosmith, A. Remnant, S. P. Perkins and H. J. Coles, *Ferroelectrics*, 2000, **243**, 75.
- T. Murias, A. C. Ribeiro, D. Guillon, D. Shoosmith and H. J. Coles, *Liq. Cryst.*, 2002, **29**, 627.
- H. J. Coles, H. Owen, J. Newton and P. Hodge, *Liq. Cryst.*, 1993, **15**, 739.
- K. Sunohara, K. Takatoh and M. Sakamoto, *Liq. Cryst.*, 1993, **13**, 283.
- J. Newton, H. Coles, P. Hodge and J. Hannington, *J. Mater. Chem.*, 1994, **4**, 869.
- H. Poths, E. Wischerhoff, R. Zentel, A. Schönfeld, G. Henn and F. Kremer, *Liq. Cryst.*, 1995, **18**, 811.
- M. Ibn-Elhaj, A. Skoulios, D. Guillon, J. Newton, P. Hodge and H. J. Coles, *J. Phys. II*, 1996, **6**, 271.
- E. Corsellis, D. Guillon, P. Kloess and H. Coles, *Liq. Cryst.*, 1997, **23**, 235.
- W. K. Robinson, C. Carboni, P. Kloess, S. P. Perkins and H. J. Coles, *Liq. Cryst.*, 1998, **25**, 301.
- J. Naciri, J. Ruth, G. Crawford, R. Shashidhar and B. R. Ratna, *Chem. Mater.*, 1995, **7**, 1397.
- J. Naciri, D. K. Shenoy, P. Keller, S. Gray, K. Crandall and R. Shashidhar, *Chem. Mater.*, 2002, **14**, 5134.
- J. Z. Vlahakis, K. E. Maly and R. P. Lemieux, *J. Mater. Chem.*, 2001, **11**, 2459.
- J.-C. Dubois, P. Le Barny, M. Mauzac and C. Noel, in *Handbook of Liquid Crystals*, ed. D. Demus, J. W. Goodby, G. W. Gray, H.-W. Spiess and V. Vill, Wiley-VCH, Weinheim, 1998, vol. 3, p. 207.
- R. P. Lemieux, *Acc. Chem. Res.*, 2001, **34**, 845.
- C. S. Hartley, C. Lazar, M. D. Wand and R. P. Lemieux, *J. Am. Chem. Soc.*, 2002, **124**, 13513.
- C. S. Hartley, N. Kapernaum, J. C. Roberts, F. Giesselmann and R. P. Lemieux, *J. Mater. Chem.*, 2006, **16**, 2329.
- M. S. Spector, P. A. Heiney, J. Naciri, B. T. Weslowski, D. B. Holt and R. Shashidhar, *Phys. Rev. E*, 2000, **61**, 1579.
- J. Naciri, C. Carboni and A. K. George, *Liq. Cryst.*, 2003, **30**, 219.
- O. E. Panarina, Y. P. Panarin, J. K. Vij, M. S. Spector and R. Shashidhar, *Phys. Rev. E*, 2003, **67**, 051709.
- N. Hayashi, T. Kato, A. Fukuda, J. K. Vij, Y. P. Panarin, J. Naciri, R. Shashidhar, S. Kawada and S. Kondoh, *Phys. Rev. E*, 2005, **71**, 041705.
- O. E. Panarina, Y. P. Panarin, F. Antonelli, J. K. Vij, M. Reihmann and G. Galli, *J. Mater. Chem.*, 2006, **16**, 842.
- J. P. F. Lagerwall, F. Giesselmann and M. D. Radcliffe, *Phys. Rev. E*, 2002, **66**, 031703.
- M. D. Radcliffe, M. L. Brostrom, K. A. Epstein, A. G. Rappaport, B. N. Thomas, R. Shao and N. A. Clark, *Liq. Cryst.*, 1999, **26**, 789.
- J. P. F. Lagerwall and F. Giesselmann, *ChemPhysChem*, 2006, **7**, 20.
- S. J. Cowling, J. W. Goodby, A. W. Hall, G. Y. Cosquer and S. Sia, presented at 10th Conference on Ferroelectric Liquid Crystals, Stare Jablonki, Poland, September 2005.
- A. de Vries, *J. Chem. Phys.*, 1979, **71**, 25.
- In each case, C_{dV} values were calculated using the maximum d_A value at T_C .
- M. Rössle, R. Zentel, J. P. F. Lagerwall and F. Giesselmann, *Liq. Cryst.*, 2004, **31**, 883.